

1 Graphical Abstract

2 **A Dynamic Evolutionary Multi-Objective Virtual Machine Place-**
3 **ment Heuristic for Cloud Data Centers**

4 Ennio Torre, Juan J. Durillo, Vincenzo de Maio, Prateek Agrawal, Shajulin
5 Benedict, Nishant Saurabh, Radu Prodan

6 Highlights

7 **A Dynamic Evolutionary Multi-Objective Virtual Machine Place-** 8 **ment Heuristic for Cloud Data Centers**

9 Ennio Torre, Juan J. Durillo, Vincenzo de Maio, Prateek Agrawal, Shajulin
10 Benedict, Nishant Saurabh, Radu Prodan

- 11 • Multi-objective algorithm for virtual machine (VM) placement in Cloud
12 data centers;
- 13 • Approximation of Pareto optimal set of VM placements;
- 14 • Resource overcommitment, resource wastage and live migration energy
15 tradeoff;
- 16 • Island-based optimisation heuristic based on genetic NSGA-II algorithm;
- 17 • Improved evaluation results compared to state-of-the-art heuristics.

18 A Dynamic Evolutionary Multi-Objective Virtual
19 Machine Placement Heuristic for Cloud Data Centers

20 Ennio Torre, Juan J. Durillo^a, Vincenzo de Maio^b, Prateek Agrawal^c,
21 Shajulin Benedict^d, Nishant Saurabh, Radu Prodan^e

22 ^a*Leibniz Supercomputing Center, Munich, Germany*

23 ^b*Vienna University of Technology, Vienna, Austria*

24 ^c*Lovely Professional University, Punjab, India*

25 ^d*Indian Institute of Information Technology, Kottayam, India*

26 ^e*University of Klagenfurt, Austria*

27 **Abstract**

Minimizing the resource wastage reduces the energy cost of operating a data center, but may also lead to a considerably high resource overcommitment affecting the Quality of Service (QoS) of the running applications. The effective tradeoff between resource wastage and overcommitment is a challenging task in virtualized Clouds and depends on the allocation of virtual machines (VMs) to physical resources. We propose in this paper a multi-objective method for dynamic VM placement, which exploits live migration mechanisms to simultaneously optimize the resource wastage, overcommitment ratio and migration energy. Our optimization algorithm uses a novel evolutionary meta-heuristic based on an island population model to approximate the Pareto optimal set of VM placements with good accuracy and diversity. Simulation results using traces collected from a real Google cluster demonstrate that our method outperforms related approaches by reducing the migration energy by up to 57% with a QoS increase below 6%.

28 *Keywords:* VM placement, multi-objective optimisation, resource

29 overcommitment, resource wastage, live migration, energy consumption,
30 Pareto optimal set, genetic algorithm, data center simulation

31 **1. Introduction**

32 Virtualized data centers are the backbone of many Cloud providers like
33 Amazon and Google that rent their physical Infrastructure-as-a-Service (IaaS)
34 to their customers. In a virtualized data center, *Virtual Machines (VMs)*
35 wrap customer applications, representing their execution environment hosted
36 onto data center *Physical Machines (PMs)*. The *VM placement* problem aims
37 to find an allocation or mapping of a set of VMs onto a subset of available
38 PMs that optimizes one or more objectives relevant to the IaaS provider.
39 More specifically, if the aim is to minimize the size of this PM subset, we
40 refer to this problem as the *VM consolidation*. This problem gathered atten-
41 tion in the last decade thanks to its ability to minimize not only the *resource*
42 *wastage*, but also the *energy consumption* and the overall electricity cost by
43 turning unused PMs to a lower power state.

44 *1.1. Motivation 1: VM overcommitment*

45 Despite these benefits, data center operators take a cautious attitude
46 towards consolidation. One approach allocates the VMs according to their
47 resource requests (i.e. CPU, memory, disk) such that the cumulative demand
48 is lower than the PMs' resource capacity. However, this suffers from *over-*
49 *provisioning* [9], as IaaS customers tend to overestimate their VM resource
50 requests to ensure fulfillment of their application requirements at all times.
51 This results in a low consolidated data center with underutilized PMs.

52 A solution to overprovisioning is to optimize the VM placement according
 53 to the VMs resource demands independently of their requests. One technique
 54 called *resource overcommitment* [10] allows placing (or consolidating) more
 55 VMs onto the same PM by sharing hardware resources exceeding its physical
 56 capacity. Unfortunately, overcommitment can have a detrimental impact on
 57 the performance of applications [6] by congesting limited PM resources with
 58 significant Quality of Service (QoS) violations and penalties.

59 To verify our motivation, we sim-
 60 ulated 100 VMs (using the homo-
 61 geneous experimental scenario de-
 62 scribed in Section 7.1) with appli-
 63 cation workloads generated by ran-
 64 domly sampling the Google cluster
 65 traces [35] using a Poisson distribu-
 66 tion. We studied the effects of the
 67 overcommitment ratio (i.e. the ra-
 68 tio between the requested and the

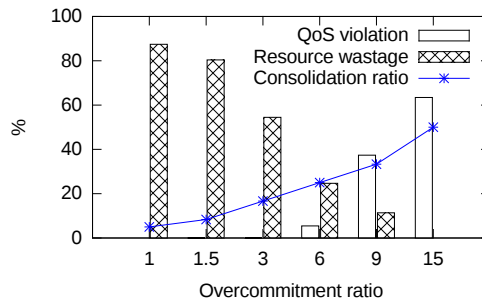


Figure 1: Impact of overcommitment on resource wastage and QoS.

69 available resources on each PM) to three important metrics: resource
 70 wastage, consolidation ratio (i.e. the ratio between the number of VMs and
 71 the allocated PMs) and QoS violation (i.e. the percentage of VMs that do
 72 not receive sufficient PM resources). Fig. 1 shows that the benefits of the
 73 overcommitment to the resource wastage decreases from 87% in case of no
 74 overcommitment, to 0% for the highest overcommitment ratio. Contrarily,
 75 the consolidation ratio increases from 5% to 50%. On the negative side,
 76 overcommitment comes with an increase in QoS violations which, although

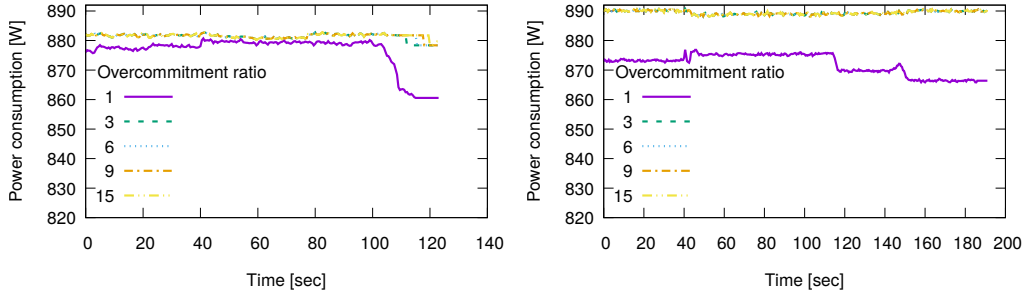
77 negligible for a low overcommitment ratio (from 1 to 6), reach a serious 60%
78 value for the highest overcommitment. It is therefore clear that the relation
79 between the resource wastage and the overcommitment ratio is crucial for
80 an energy-efficient resource management under QoS constraints, Moreover,
81 understanding this relation is not immediate due to the conflicting nature of
82 the two objectives leading to a wide spectrum of different possible tradeoffs.

83 1.2. Motivation 2: live VM migration

84 Dynamic real-world VM workloads require continuous on-the-fly modifi-
85 cations of the VM placements, supported through *VM migrations* and en-
86 abling different potential resource overcommitment and wastage tradeoffs.
87 To minimize the impact on the application QoS, *live migration* transpar-
88 ently moves a running VM between different PMs without disconnecting it
89 from the client and exposing no (or minimum) interruptions.

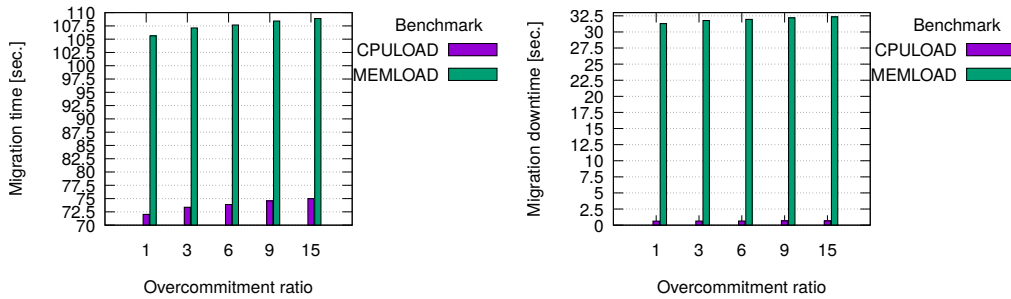
90 The cost of VM migration has two main dimensions [18]: the *downtime*
91 (i.e. VM unavailability) and the additional power consumption on the source
92 and target PMs during this process. To understand the impact of overcom-
93 mitment on these parameters, we conducted an experiment that measures the
94 VM energy consumption and its migration time on an overcommitted PM
95 using the same VM workload as in Section 1.1 on the machines presented in
96 Table 1. We further generated two VM-internal CPU and memory-intensive
97 workloads that influence its live migration, as described in [19]:

- 98 • CPULOAD uses OpenMP implementation of a matrix multiplication algo-
99 rithm running on all cores allocated to the VM.
- 100 • MEMLOAD continuously updates the VM memory pages using a high 95%



(a) Instantaneous CPULOAD power.

(b) Instantaneous MEMLOAD power.



(c) Migration time versus overcommitment.

(d) Downtime versus overcommitment.

Figure 2: Impact of overcommitment on VM power consumption, migration time and downtime for CPU and memory-intensive workloads.

101 dirtying rate (i.e. percentage of memory pages that become dirty in a
 102 given interval), considered as the most impacting factor on downtime [3].

103 Fig. 2a and Fig. 2b show that the overcommitment ratio (especially above
 104 three) does not affect the power consumption of the source PM. The drop in
 105 power in the absence of overcommitment after around 100s in Fig. 2a and
 106 120s in Fig. 2b is due freeing the source PM resources. However, Fig. 2c
 107 shows that the overcommitment has an impact on the VM migration time
 108 and affects its energy consumption. For this reason, we separately consider

109 the VM migration energy from server energy consumption.

110 Fig. 2d shows the CPULOAD downtime ranges between 300 ms to 600 ms,
111 which is negligible according to [3]. The MEMLOAD downtime is up to 30
112 the case of an extreme 95% dirtying rate. Since our experimental workloads
113 exhibit a dirtying rate below 15% for all the tasks with a downtime below
114 1 s, we define the VM migration cost in term of its energy consumption only.

115 Finally according to [31], the energy overhead may be up to 2.5 kJ for
116 each VM migration, accounting for 10% of the idle energy consumption of
117 an average PM. Furthermore, the energy overhead of VM migration can be
118 as high as 5.8% of total energy consumption of a data center [2]. Therefore,
119 understanding the impact of migrations on the other metrics is important,
120 since they influence other aspects of data centre operation.

121 1.3. Problem statement

122 To address these motivations, we propose a *multi-objective method* and
123 algorithm for dynamic placement of VMs in response to their fluctuating
124 resource demands. Our goal is to minimise the energy consumption in data
125 centres faced with dynamic workloads by dynamically allocating VMs to
126 the minimum number of PMs using a three-fold strategy: 1) reduce the
127 number of PMs by increasing the overcommitment; 2) analyse the effects
128 of the overcommitment and overly reduced number of PMs on the QoS;
129 3) analyse the effects on live migration, ignored in related work.

130 We model the VM placement as a multi-objective *Vector Bin Pack-*
131 *ing (VBP)* [15] problem considering three conflicting objectives: resource
132 wastage, overcommitment ratio, and migration cost. We introduce a novel
133 *island-based evolutionary meta-heuristic* that dynamically provides a set of

134 tradeoff VMs placements that accommodate the workload demand. Contrary
135 to single solution approaches, we demonstrate the advantage of approximat-
136 ing the entire set of “optimal” tradeoff placements through simulation results
137 on real-world traces obtained from a Google cluster. Such a multi-objective
138 approach is an asset that reveals tradeoff placements from the search space
139 not covered by single-objective approaches and impossible to see otherwise.

140 *1.4. Article structure*

141 The next section discusses the related work, followed by a multi-objective
142 optimization background in Section 3. We introduce and formalize the VM
143 placement problem in Section 4, [implemented in practice within the archi-](#)
144 [tecture of a dynamic Cloud computing environment for real-world scientific](#)
145 [and industrial workloads, presented in Section 5](#). We present an island-based
146 evolutionary meta-heuristic for solving the VM placement problem in Sec-
147 tion 6. Section 7 evaluates our method compared to related approaches on
148 real data center simulation traces. Section 8 concludes the paper.

149 **2. Related Work**

150 We classify the studies on dynamic VM placement in two categories:
151 single and multi-objective approaches.

152 *2.1. Single-objective placement*

153 In contrast to our multi-objective approach, these works are limited to
154 approximating a single optimized placement solution.

155 First Fit Decreasing (FFD) is a fundamental algorithm used in the com-
156 munity for benchmarking VM placement algorithms. FFD sorts the VMs

157 according to their CPU and memory size in descending order, and sequen-
158 tially places them on the first PM with sufficient resources. MM_MBFD [7]
159 is a two phase algorithm that combines a minimisation of migration (MM)
160 algorithm that selects the VMs to migrate based on a double-CPU threshold
161 policy with a modified best-fit decreasing (MBFD) VM placement heuristic
162 to keep the total CPU demand of the placed VMs between the two thresholds.

163 Murtazaev et al. [25] proposed a method that reduces the number of
164 active PMs by iteratively migrating the VMs from the least loaded to the
165 more loaded ones. Verma et al. [34] introduced an algorithm that mini-
166 mizes the number of migrations and the energy cost by first computing the
167 placement that minimizes the power consumption, then calculating the mi-
168 grations required to modify the current placement, and finally migrating the
169 VMs with the minimum ratio between the estimated power consumption
170 and the migration cost. Van et al. [33] implemented a method for power and
171 performance-efficient provisioning of VMs and PMs by using a utility func-
172 tion for the optimal tradeoff between energy and performance. Beloglazov
173 et al. [7] proposed a method that initially determines the minimum number
174 of migrating VMs for keeping the PMs' utilization within a certain interval,
175 followed by a modified FFD placement algorithm. Takahashi et al. [32] pre-
176 sented a greedy heuristic to minimize the total power consumption and the
177 performance degradation due to VM consolidation. Mi et al. [22] proposed
178 a proactive VM placement reconfiguration method based on predicted appli-
179 cation demand using a modified genetic algorithm that minimizes the overall
180 PM power consumption and maximizes the utilization. Ferdous et al. [14]
181 implemented a colony optimization meta-heuristic for finding a dynamic VM

182 placement that balances the load among the the minimum number of PMs
183 and minimizes the power consumption. All these works provided QoS guar-
184 antees by constraining the PM utilization achievable by a VM placement.

185 Other approaches look at the tradeoff between power consumption and
186 performance degradation, but transform the problem into a single objective
187 one by using a utility function or a weighted sum of the objectives. However,
188 weighting and combining incompatible metrics in a single arithmetic function,
189 despite being artificial and unrealistic, is an a-priori method with unclear
190 impact on the solution. Li et al. [17] modeled the VM placement as a mixed
191 integer linear programming problem that optimizes application performance,
192 license cost and power consumption. Xu et al. [36] built a controller that
193 places the VMs with optimized temperature, performance and power.

194 *2.2. Multi-objective placement*

195 Similar to our approach, several works focused on the simultaneous opti-
196 mization of multiple objectives.

197 Lama et al. [16] built an analytic queuing model simulated as a multi-
198 objective problem that minimizes the response time and the number of PMs
199 and VMs of an n -tier application using the NSGA-II algorithm [11] and a
200 stress-strain decision making strategy. Contrary to [16], our approach does
201 not focus on a particular workload type (i.e. three-tier applications), but
202 considers heterogeneous workloads including the migration cost incurred by
203 placement modifications (ignored in [16]).

204 Sallam at al. [30] proposed a migration policy that selects a VM from a
205 given set based on the migration cost, resources wastage, power consumption,
206 thermal dissipation, and PM load. Our approach also accounts for migration

207 cost and resource wastage, however, our goal is to dynamically optimise the
208 VM placements, while [30] focuses on selecting the “optimal” VM to migrate.

209 To the best of our knowledge, our work is the first to exploit the con-
210 flict between resource overcommitment and wastage represented as a tradeoff
211 between energy consumption and performance metrics.

212 3. Background

213 3.1. Vector Bin Packing

214 We theoretically model the VM placement as a *Vector Bin Packing (VBP)*
215 problem, which maps a set of VMs with known resource demands onto a set of
216 PMs with known resource capacities [24]. The demands of the VMs and the
217 capacities of the PMs are v -dimensional vectors, whose components represent
218 v resource types, such as CPU number, memory size, disk space, or network
219 bandwidth. VBP’s goal is to place the VMs onto the minimum number of
220 PMs, such that the cumulative demand of the VMs sharing the same PM is
221 smaller than or equal to its capacity in each dimension.

222 Fig. 3a gives a VM placement example across two resources: CPU and
223 memory. The inner dotted line represents the resource capacity of a single
224 PM, while the dimensions of the small rectangles indicate the two resource
225 demand dimensions of six VMs. After placing the VMs in a vector fashion,
226 their aggregated resource demand determines the wastage in each dimension.
227 Fig. 3b shows an overcommitment example due to load fluctuations of the
228 VMs allocated in Fig. 3a and requiring more physical resources than the
229 total PM capacity. The virtualization technology copes with the overcom-
230 mitment by multiplexing the PM resources shared among VMs, as shown

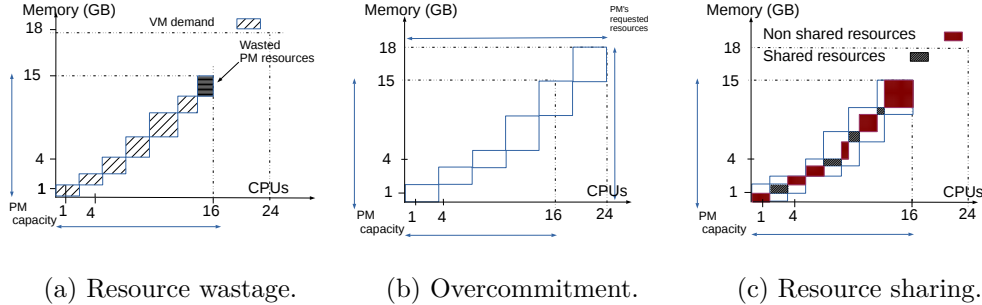


Figure 3: VBP allocation of six VMs onto one PM with 16 CPUs and 15 GB of memory.

231 by the red-shaded rectangles in Fig. 3c. Resource sharing increases with the
 232 overcommitment ratio and degrades the performance.

233 Our method generalizes the original VBP by dealing with overcommit-
 234 ment and treating VM placement as a dynamic problem. In our model,
 235 VMs have a static size and a variable resource demand described by two
 236 v -dimensional vectors. PMs have an associated resource wastage, an over-
 237 commitment ratio and a VM migration cost. While the resource wastage
 238 and the overcommitment ratio depend on the demand and on the size of
 239 the placed VMs, the migration cost depends on the energy consumption re-
 240 quired to modify a placement. Our goal is to simultaneously optimize the
 241 PMs’ resources wastage, overcommitment ratio, and migration cost, which
 242 are conflicting objectives that require multi-objective optimization.

243 3.2. Multi-objective optimization

244 A *multi-objective optimization* problem consists of a vector of k objective
 245 functions $\overrightarrow{f(\vec{x})} = (f_1(\vec{x}), f_2(\vec{x}), \dots, f_k(\vec{x}))$. These objectives are usually
 246 in conflict with each other, meaning that optimizing one implies worsening at

247 least another one. Without loss of generality, we consider the minimization of
248 all functions. The next section describes objectives considered in this work.

249 The components of a solution vector (or simply solution) $\vec{x} = (x_1, \dots, x_n)$
250 are *decision variables*. The set of all possible solutions is called the *search*
251 *space* S . In our case, each decision variable corresponds to a VM. The i^{th}
252 decision variable represents the identifier of the PM used for mapping the i^{th}
253 VM. Therefore, a *solution* represents a mapping of all the VMs placed onto
254 the available PMs. The set of all possible mappings is the search space S .

255 A solution \vec{x}_1 *dominates* another solution \vec{x}_2 (or mathematically $\vec{x}_1 \preceq \vec{x}_2$)
256 if it is better in at least one objective and not worse in the rest: $f_i(\vec{x}_1) \leq$
257 $f_i(\vec{x}_2), \forall i \in [1, n]$, and $\exists j \in [1, n]$ such that $f_j(\vec{x}_1) < f_j(\vec{x}_2)$.

258 The solution of a multi-objective optimization problem is a set of non-
259 dominated solutions representing a tradeoff among the objective functions.
260 The set of tradeoff solutions non-dominated by any other solution in S is
261 called *Pareto optimal set*, and the objective values of the solutions in the
262 Pareto optimal set defines the *Pareto frontier*. A Pareto frontier usually
263 consists of an infinite set of points whose computation is an NP-complete
264 problem. The goal of a multi-objective optimization is to approximate the
265 Pareto optimal set by maximizing two properties: (1) *convergence* by being
266 as close as possible to the Pareto frontier, and (2) *diversity* by uniformly
267 covering the range of tradeoff solutions in the Pareto frontier.

268 3.3. NSGA-II

269 Evolutionary algorithms are popular techniques to approximate the Pareto
270 frontier of a multi-objective optimization problem. Among them, NSGA-II [11]
271 is the most popular and well-known in the literature, presented in Algo-

272 rithm 1. NSGA-II works with a population T of N candidate solutions,
 273 initialized in line 1 and improved in convergence and diversity in an itera-
 274 tive process (lines 3 – 14). In each iteration, the algorithm generates a new
 275 set Q of solutions (line 9) by means of two operations: crossover (line 7)
 276 and mutation (line 8). These operations have their inspiration in the the-
 277 ory of species evolution, and try to exploit the content of T to seek higher
 278 quality solutions. The set $R = T \cup Q$ (line 11) generates the population T
 279 for the next iteration and uses the `rankingAndCrowding` function (line 12)
 280 to arranges the population in different fronts. The first front contains non-
 281 dominated solutions, the second front contains only solutions dominated by
 282 the first front, and so on. Each front sorts the solutions according to a density
 283 measurement metric called *crowding distance* [11] to ensure diversity. The
 284 `selectBestIndividuals` function finally selects the best N individuals from
 285 R (line 13) aiming to converge towards the Pareto frontier. The algorithm
 286 repeats these steps until reaching a termination condition (line 3).

287 4. Model and Problem Statement

288 We present the resource model and the objective functions of our method.

289 4.1. Physical machines (PMs)

290 We consider a data center composed of m PMs $P = \{p_1, \dots, p_m\}$. A
 291 *resource capacity vector* $\overrightarrow{CV}(p) = (c_1, \dots, c_v)$ describes each PM $p \in P$,
 292 where every dimension $k \in [1, v]$ indicates the capacity of each PM phys-
 293 ical resource r_k in the set $R = \{r_1, \dots, r_v\}$. In a typical Cloud scenario,
 294 $R = \{CPU, memory, disk, network\}$, abstracted by the virtualization tech-

Algorithm 1: NSGA-II algorithm

```
1  $T \leftarrow \text{initializePopulation}()$  ;           // Initial population.
2  $R \leftarrow \emptyset$  ;                       // Auxiliary population.
3 while  $\text{terminationCondition}()$  do
4    $Q \leftarrow \emptyset$  ;                     // Offspring population.
5   for  $i \leftarrow 1$  to  $\frac{\text{populationSize}}{2}$  do
6      $\text{parents} \leftarrow \text{selection}(T)$ 
7      $\text{offspring} \leftarrow \text{crossover}(\text{parents})$ 
8      $\text{offspring} \leftarrow \text{mutation}(\text{offspring})$ 
9      $Q \leftarrow \text{offspring}$ 
10  end
11   $R \leftarrow T \cup Q$ 
12   $\text{rankingAndCrowding}(R)$  ;                 // Population sorting.
13   $T \leftarrow \text{selectBestIndividuals}(R)$ 
14 end
```

Result: Non-dominated solutions from T .

295 nology [5]. Our study focuses on CPU and memory, as the most overcom-
296 mitted resources in data centers and strongly affect the VM migration [19].

297 4.2. Virtual machines (VMs)

298 We identify two sets of VMs that participate in the placement process.
299 The *incoming VMs* are new VMs that scale up applications or create new
300 application deployments. The *hosted VMs* are the currently running ones.
301 All together, they define a set $VM = \{vm_1, \dots, vm_n\}$ placed on an optimized
302 subset of PMs $P_{used} \subseteq P$. Each $vm \in VM$ has two v -dimensional vectors.

303 *Resource size vector.* $\overrightarrow{SV}(vm) = (s_1, \dots, s_v)$ indicates the amount s_k of the
 304 resource r_k requested by the VM vm , with $k \in [1, v]$;

305 *Resource demand vector.* $\overrightarrow{DV}(vm, t) = (d_1(t), \dots, d_v(t))$ defines the vm 's
 306 workload demand $d_k(t)$ for each resource r_k at time instance t , with $k \in [1, v]$.

307 4.3. VM placement objectives

308 We defined in Section 3.2 a placement of n VMs as $\vec{x} = (x_1, \dots, x_n)$,
 309 where each decision variable x_i maps the i^{th} VM $vm_i \in VM$ to a PM $p \in P$.
 310 Given \vec{x} , we further define the set of VMs allocated on the same PM $p \in P$
 311 as follows: $\delta(p, \vec{x}) = \{vm_i \in VM \mid x_i == p\}$.

312 To facilitate the VBP problem formulation, we normalize (to values in the
 313 space $[0, 1]^v$) the vector $\overrightarrow{CV}(p)$ with respect to the resource capacity of the
 314 PM p , and the vectors $\overrightarrow{SV}(vm)$ and $\overrightarrow{DV}(vm, t)$ with respect to the capacity
 315 of the PM hosting the VM vm . We define in the following the three objective
 316 functions targeted by our optimization process.

317 4.3.1. Objective 1: resource wastage

318 The first objective function f_1 quantifies the resource wastage over each
 319 v resource dimension entailed by a placement \vec{x} . We define the *cumulative*
 320 *demand vector* for a machine p at instant of time t as:

$$\overrightarrow{CDV}(p, t, \vec{x}) = \sum_{vm \in \delta(p, \vec{x})} \overrightarrow{DV}(vm, t).$$

321 This vector aggregates the resource demands of all VMs placed on a PM p at
 322 time instance t . If the components of $\overrightarrow{CDV}(p, t, \vec{x})$ are larger than the ones
 323 in the resource capacity vector $\overrightarrow{CV}(p)$ at any time instance t , the cumulative
 324 demand exceeds the PM capacity and the VMs contend for PM resources.

325 We define the *resource wastage vector* for a machine p at instance t as:

$$\overrightarrow{WV}(p, t, \vec{x}) = \overrightarrow{CV}(p) \ominus \overrightarrow{CDV}(p, t, \vec{x}),$$

326 where the operation \ominus has the following definition:

$$\vec{A} \ominus \vec{B} = (\max(A_1 - B_1, 0), \dots, \max(A_v - B_v, 0)).$$

327 This vector indicates the amount of unused resources in each dimension.

328 When $\overrightarrow{CDV}(p, t, \vec{x})$ is larger than $\overrightarrow{CV}(p)$ in one dimension, we set $\overrightarrow{WV}(p, t, \vec{x})$

329 to 0 in that dimension, as the resource has 100% utilisation and no wastage.

330 We define the *total wastage vector* at time instance t as the sum of the

331 resource wastage vectors of across all used PMs:

$$\overrightarrow{TWV}(\vec{x}, t) = \sum_{p \in P_{used}} \overrightarrow{WV}(p, t).$$

332 We finally define the resource wastage f_1 as the magnitude of the total

333 wastage vector:

$$f_1(\vec{x}) = \|\overrightarrow{TWV}(\vec{x}, t)\|.$$

334 4.3.2. Objective 2: overcommitment ratio

335 The second objective function f_2 measures the *overcommitment ratio*, as

336 the percentage of PM resources requested by VMs in excess to their capacity.

337 Given a placement \vec{x} , the overcommitment ratio f_2 adds all the normalized

338 resources size vectors $\overrightarrow{SV}(vm) = (s_1, \dots, s_v)$ of all the VMs divided by the

339 number of PMs in use:

$$f_2(\vec{x}) = \frac{\sum_{p \in P_{used}} \sum_{vm \in \delta(p, \vec{x})} \sum_{i=1}^v s_i}{|P_{used}|},$$

340 where $P_{used} = \{p \in P \mid \delta(p, \vec{x}) \neq \emptyset\}$.

341 *4.3.3. Objective 3: migration cost*

342 The third objective f_3 estimates the *migration cost* triggered by a place-
 343 ment \vec{x}' . Following the experimental motivation from Section 1.2, we calcu-
 344 late the VM migration cost as its energy consumption considering the page
 345 dirtying rate and the load of the source p_{src} and target p_{trg} PMs [18, 19]:

$$P(vm, p_{src}, p_{trg}, t) = P(vm, p_{src}, t) + P(vm, p_{trg}, t).$$

346 Therefore, the energy consumption of migrating a VM vm on a PM p is:

$$E(vm, p) = \int_{t_{start}}^{t_{stop}} P(vm, p, t) dt,$$

347 where $t_{stop} - t_{start}$ is the duration of the migration, as defined in [18]. Given
 348 a current placement of n VMs $\vec{x} = (x_1, \dots, x_n)$, the cost of migrating them
 349 to a new placement $\vec{x}' = (x'_1, \dots, x'_n)$ is:

$$f_3(\vec{x}) = \sum_{\substack{i \in [1, n] \wedge \\ x_i \neq x'_i}} E(vm_i, x_i) + E(vm_i, x'_i).$$

350 **5. Dynamic VM Placement in Cloud Data Centers**

351 In this section, we first describe the overall software architecture hosting
 352 our dynamic VM placement method, implemented in practice as part of the
 353 ASKALON Cloud computing environment [13]. Afterwards, we give illustra-
 354 tive examples of typical VM workloads under its operation that benefit from
 355 our approach. Finally, we describe the dynamic VM placement algorithm.

356 *5.1. ASKALON Cloud Computing Environment for Real-World Scientific
 357 and Industrial Workloads*

358 We carry out this research as part of the ASKALON [13] application
 359 development and computing environment for scientific and industrial appli-

360 cations on distributed high-performance Cloud infrastructures. ASKALON
361 supports the scientists and engineers in designing applications as independent
362 tasks or workflows through a number of services that transparently execute
363 them as VMs onto the underlying heterogeneous PMs, as follows:

- 364 1. *Execution Engine* is responsible for processing the incoming tasks and
365 prepares them for scheduling, deployment and execution;
- 366 2. *Monitoring* service observes the infrastructure workload and provides
367 useful utilization metrics to the other services;
- 368 3. *Multi-objective optimisation* applies techniques like the Island NSGA-II
369 proposed in this paper (see Section 6) and identifies the “best” VM to
370 PM mappings based on the user objectives (see Section 4.3);
- 371 4. *Decision making* is a manual or automatic procedure that selects the
372 preferred mapping from the set of Pareto optimal mappings;
- 373 5. *Dynamic VM placement* uses a simple iterative algorithm to deploy the
374 tasks wrapped in optimised VMs onto the PMs selected by the decision
375 making service (see Section 5.3);
- 376 6. *Resource management* optionally allocates or releases resources to min-
377 imize the number of active PMs.

378 We successfully applied ASKALON over the the last two decades together
379 with various domain scientists for running computational intensive workloads
380 on a number of applications, including computational chemistry, meteorol-
381 ogy, astrophysics, graphics rendering, and online games.

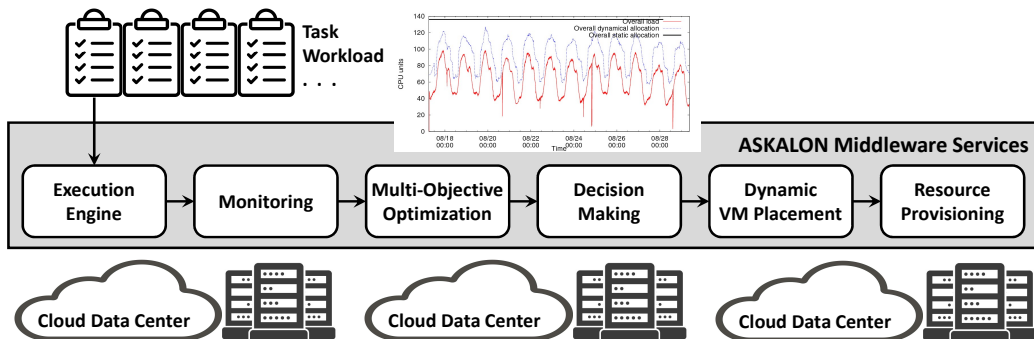


Figure 4: ASKALON Cloud computing architecture.

382 *5.2. Illustrative Target Workload Examples*

383 We target elastic predictable workloads running on data centers, such
 384 as periodic workloads. Periodic workloads are common in real-world, for
 385 example in business applications performing (monthly, yearly) auditing or
 386 balance computations, in transportation systems experiencing typical rush
 387 hours and idle times (during night), and in massively multiplayer online game
 388 (MMOG) servers with high player activity during afternoon and low numbers
 389 of connected player after midnight up (to early morning) [26].

390 Our design follows a successful preliminary work on dynamic resource pro-
 391 visioning and VM placement for MMOGs, which achieved a 250% improve-
 392 ment in resource provisioning for RuneScape [26]. To guarantee a seamless
 393 interaction to all players at all times, we triggered in this work a simple
 394 dynamic VM placement algorithm (based on resource matchmaking) with
 395 a high frequency of two minutes using a low overhead live migration func-
 396 tionality with a low impact on the QoS below 3%. In such scenarios, the
 397 infrastructure operators typically perform dynamic resource management at
 398 regular intervals (e.g. hourly) to optimize their utilization, depending on

Algorithm 2: Dynamic VM placement algorithm.

Input : $P = \{p_1, \dots, p_m\}$; // Set of PMs
Input : $VM_0 = \{vm_1, \dots, vm_n\}$; // Initial set of VMs
Input : \vec{x}_0 ; // Initial placement
1 $t \leftarrow 0$
2 $\vec{x} \leftarrow \vec{x}_0$
3 **while** $t \leq t_{end}$ **do**
4 $VM_{t+1} \leftarrow VM_t + VM_{new}$; // New VM set
5 $S \leftarrow \text{Island-NSGAI}(\mathit{P}, VM, \vec{x})$; // Pareto optimal set
6 $\vec{x} \leftarrow \text{decisionMaking}(S)$; // Preferred solution
7 $t \leftarrow t + 1$; // Next time instance
8 **end**

399 historical variable resource use at specific times of the day, week, month
400 or year. Within a certain provisioning interval, the operators perform occa-
401 sional adaptive VM placements depending on the dynamic CPU and memory
402 load exhibited by individual VMs. The appropriate VM placement interval
403 is workload dependent and can range from minutes to hours, days or longer.

404 5.3. Dynamic VM Placement Algorithm

405 Algorithm 2 describes our dynamic VM placement method with three
406 input parameters: 1) the set P of PMs in the data center described by
407 their capacity vector \vec{CV} , 2) the initial set of VMs VM described by their
408 resource size \vec{SV} and demand After approximating the Pareto frontier, a
409 **decisionMaking** function selects in line 6 a preferred tradeoff VM placement.
410 This procedure can be either manual or automatic based on environment-

411 specific rules or constraints defined by the resource provider, such as min-
 412 imizing the wastage without QoS violations or keeping VM migration cost
 413 bellow a server energy fraction. \overrightarrow{DV} vectors, and 3) an initial placement \overrightarrow{x}_0
 414 representing the initial state of the data center. The algorithm iterates over
 415 a series of timestamps to periodically optimize the VM placements according
 416 to the time-varying VM resource demands (lines 3–8). At each timestamp, it
 417 merges the set of incoming VMs VM_{new} with the already hosted ones VM_t
 418 into a new set VM_{t+1} (line 4). Afterwards, the main **IslandNSGA-II** func-
 419 tion (line 5) implemented as an evolutionary multi-objective optimization
 420 heuristic periodically computes an approximation to the Pareto optimal set
 421 of possible VM placements onto the available PMs. This approximation con-
 422 tains “optimal” tradeoffs among the three objectives described in Section 4.3.

423 6. Island NSGA-II Algorithm

424 We research in this section an evolutionary algorithm that improves the
 425 convergence and diversity of NSGA-II [11] presented in Section 3.3 to deter-
 426 mine the Pareto optimal set of tradeoff placements, modelled as a general-
 427 ization of the NP-complete VBP problem [15] (see Section 3.1). Every VM
 428 placement is a vector $\overrightarrow{x} = (x_1, \dots, x_n)$, as defined in Section 4. NSGA-II
 429 works with a population T of candidate VM placements, randomly initialised
 430 by selecting a random PM $p \in P$ for each decision variable x_i of each place-
 431 ment $\overrightarrow{x} \in T$. We employ a single-point crossover operator that selects two
 432 placements \overrightarrow{x}_1 and \overrightarrow{x}_2 from the population T , and generates a new placement
 433 \overrightarrow{x}_3 by combining the first half of \overrightarrow{x}_1 with the second half of \overrightarrow{x}_2 . The mutation
 434 operator takes the new placement created by crossover, randomly selects a

435 VM, and changes its placement to a random PM.

436 6.1. Pareto analysis

437 The generated Pareto frontier has three dimensions corresponding to the
438 three objective functions. To facilitate the analysis, we use two-dimensional
439 representations of the Pareto frontiers mapping the resource wastage (f_1) and
440 the overcommitment ratio (f_2) on one unit-less y -axis and the VM migration
441 energy (in J) on the x -axis. For example, Fig. 5 represents the overcom-
442 mitment ratio (blue cross) and resource wastage (red circle) as comparable
443 Pareto frontiers. A placement \vec{x} representing a tradeoff between a resource
444 wastage $f_1(\vec{x})$, an overcommitment ratio $f_2(\vec{x})$ and a migration energy
445 $f_3(\vec{x})$ is a (blue) cross at coordinates $(f_3(\vec{x}), f_1(\vec{x}))$ and a red circle at
446 coordinates $(f_3(\vec{x}), f_2(\vec{x}))$. We can therefore conclude that the Pareto
447 frontier in Fig. 5b provides a lower resource wastage than the one in Fig. 5a.
448 In addition, a horizontal (green) line represents the solution computed by
449 the FFD [25] introduced in Section 2.

450 Fig. 5a displays the outcome of the NSGA-II algorithm for the homo-
451 geneous scenario described in Section 7.1 at the first time instance. We
452 compute the initial VM placement \vec{x}_0 using the FFD baseline method (see
453 Section 2.1), which leads to a high resource wastage. Moreover, Fig. 5a
454 shows that NSGA-II produces solutions that do not improve much the re-
455 source wastage, even for placements involving a lot of migrations (indicated
456 by high energy consumption towards the right part of the x -axis.)

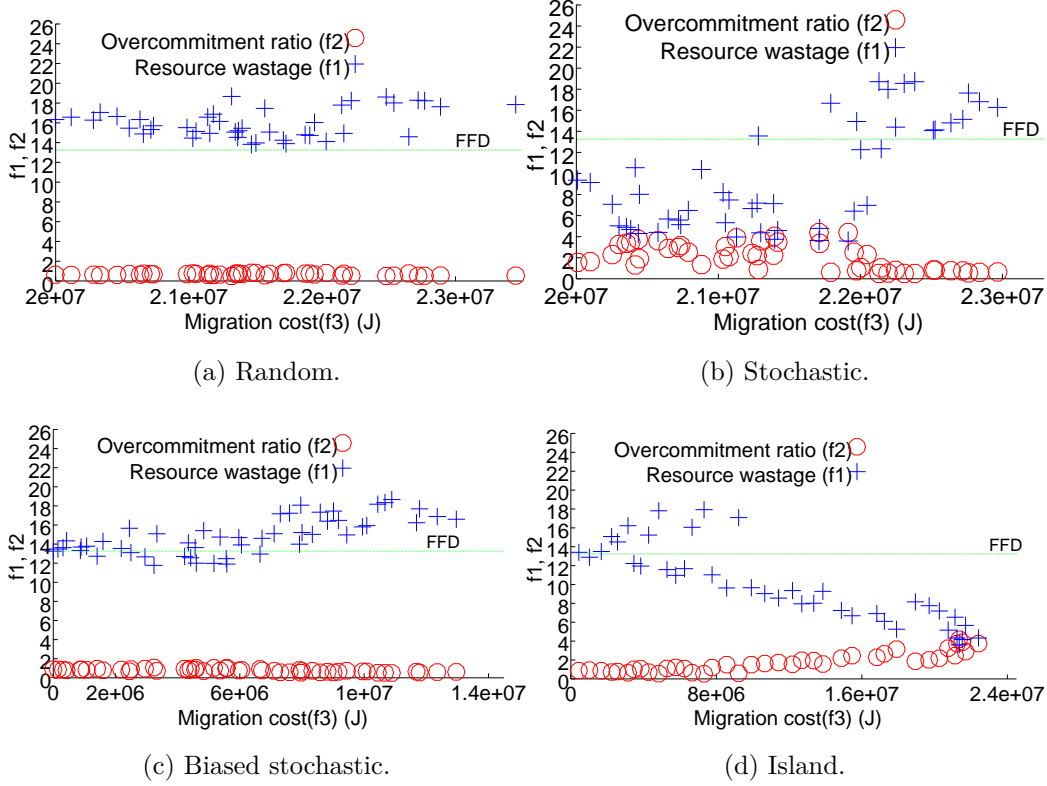


Figure 5: Pareto optimal sets for different generation methods of the initial population.

457 *6.2. NSGA-II with stochastic initial population*

458 To lower the resource wastage, we aim to improve the results of NSGA-II
 459 by initializing the population T with placements with minimum resource
 460 wastage that map all VMs onto one single PM from the set P . The idea is to
 461 start from optimal placements respect to the first objective f_1 and explore the
 462 solution space for finding better solutions with respect to resource overcom-
 463 mitment f_2 and migration cost f_3 . For generating the initial population, we
 464 first calculated the rate $\eta_p = \mathcal{F}(|\delta(p, \vec{x}_0)|, \epsilon)$ of expected placements on each
 465 PM $p \in P$, where $\eta_p, \epsilon \in (0, 1]$, $|\delta(p, \vec{x}_0)|$ is the number of VMs currently

466 placed on p , and $\sum_{p \in P} \eta_p = 1$. The parameter ϵ guarantees proportional
467 placements on a PM p , which are not present in the current placement (i.e.,
468 $|\delta(p, \vec{x}_0)| = 0$). Afterwards, we simulated a roulette wheel with $m = |P|$ slots
469 of size proportional to $\eta_p, \forall p \in P$, spun the wheel $|T|$ times, and created each
470 time a VM placement onto the winning PM p .

471 The Pareto frontier in Fig. 5b improves on the original NSGA-II algo-
472 rithm with several low resource wastage placements coming at higher over-
473 commitment and migration costs (crowded towards the right of the x -axis.)

474 6.3. NSGA-II with biased stochastic initial population

475 To lower the migration costs, we insert the current placement in T , which
476 introduces a bias towards the region of the Pareto optimal set with a low
477 migration cost. Fig. 5c shows that, although the algorithm provides solutions
478 similar to the current placement (i.e. low migration cost), they are far from
479 the stochastic approach in resource wastage (or overcommitment).

480 6.4. Island NSGA-II

481 To increase the diversity of the population and converge to wider vari-
482 ety of better solutions, we employed the island model, which conceptually
483 consists of several populations (the islands) evolving independently of each
484 other, potentially using different algorithms and occasionally exchanging in-
485 dividuals. Algorithm 5 considers two islands corresponding to the stochastic
486 and biased stochastic generation of the initial population, initialised in lines 6
487 and 7. At every iteration (lines 5 – 14), we gather the populations of each
488 island, merge them (line 8), extract the best individuals according to ranking
489 and crowding metrics [11] (line 9), and update the current population of each

Algorithm 3: Island NSGA-II algorithm.

```
Input :  $P = \{p_1, \dots, p_m\}$ ; // PM set
Input :  $VM = \{vm_1, \dots, vm_n\}$ ; // Initial VM set
Input :  $\vec{x}$ ; // Current placement
1  $T1 \leftarrow \emptyset$ ; // First island
2  $T2 \leftarrow \emptyset$ ; // Second island
3  $i \leftarrow 0$ 
4 while  $i \leq i_{\max}$ ; // Iterate for  $i_{\max}$  generations
5 do
6    $T1 \leftarrow \text{stochasticGeneration}(\vec{x}, P, VM, T1)$ 
7    $T2 \leftarrow \text{biasedGeneration}(\vec{x}, P, VM, T,)$ 
8    $Q \leftarrow T1 \cup T2$ 
9    $\text{rankingAndCrowding}(Q)$ 
10   $T \leftarrow \text{selectBestIndividuals}(Q)$ 
11   $T1 \leftarrow T$ 
12   $T2 \leftarrow T$ 
13   $i \leftarrow i + 1$ 
14 end
```

490 island accordingly. This method forces individual islands to further explore
491 solutions on the entire Pareto frontier and avoids focus on local areas only.

492 Fig. 5d shows that the island algorithm finds better tradeoff placements,
493 ranging from few migrations and similar resource wastage to many migrations
494 and substantially different wastage (or overcommitment).

495 *6.5. Complexity analysis*

496 MM_MBDF, MM_MBDF_2 and FFD have an $O(n \cdot m)$ complexity [7],
497 where m is the number of PMs and n is the number of VMs. The Island
498 NSGA-II algorithms consist of two phases. The first phase uses FFD to
499 compute an initial solution with $O(m \cdot n)$ complexity. The second phase is a
500 classical NSGA-II algorithm with a complexity of $O(o \cdot p^2)$ [11], where o is
501 the number of objectives and p is the population size. Since our problem has
502 three objectives ($m = 3$), this results in an overall complexity of $O(m \cdot n + p^2)$.
503 Related work [12] demonstrated that the population size does not need to
504 scale in the same magnitude as the decision variable vector (i.e. $p \ll n$)
505 leaving our Island NSGA-II algorithm with quadratic complexity of $O(m \cdot n)$.

506 **7. Experimental Evaluation**

507 We first evaluate our method as a decision making tool in Section 7.3.
508 Secondly, we compare it with other VM placement solutions in Section 7.4.

509 *7.1. Experimental setup*

510 We conducted the experiments using the GroudSim [28] discrete event-
511 based simulator for Cloud environments, extended to consider CPU and
512 memory overcommitment through mechanisms such as memory reclamation
513 and CPU-proportional fair scheduling [5, 27].

514 We simulated a data center with 200 PMs in two configurations displayed
515 in Table 1: (1) *homogeneous* with PMs of type M2 only, and (2) *heterogeneous*
516 four PM types (M1, M2, M3 and M4) of 50 PMs each. We set the initial
517 number of VMs to 500 and computed the initial VM placement \vec{x}_0 using the

Table 1: Experimental data center.

<i>PM type</i>	<i>Virtual CPUs</i>	<i>RAM</i>	<i>Power [idle]</i>	<i>Power [100%]</i>
M1	32 (16×Opteron 8356)	32 GB	501 W	840 W
M2	40 (10×Xeon E5-2690v2)	128 GB	164.2 W	382 W
M3	32 (8×Xeon E5-2660)	32 GB	90 W	310 W
M4	32 (8×Xeon E5-2660)	32 GB	105 W	340 W

518 basic FFD algorithm (see Section 2.1). Afterwards, we added and removed a
 519 random number of VMs at different time instances to simulate a real Cloud
 520 environment where users deploy and stop VMs in an unpredictable manner,
 521 as researched in [8].

522 We simulated one full day of data center operation in each experiment.
 523 We set the interval between two periodic Pareto frontier computations to
 524 30 min, as Google cluster traces exhibit a long-term resource demand vari-
 525 ability [29] and a stable task resource demand within an hourly time period.
 526 We selected the size and the workload of each VM using the Google cluster
 527 traces [35] containing the resource use of 25,462,157 tasks over a period of 29
 528 days. Every task run on a separate VM and requested a maximum percentage
 529 of the PM resources. After deploying a simulated VM, we randomly selected
 530 a task and determined its VM size and workload demand by the maximum
 531 requested resources and by its resource use. The number of VMs migrated at
 532 each time instance depends on the amount of CPU load [21]. Our workload
 533 is typical to Web applications, whose load ranges from 10.7 – 87.6% with
 534 62.8% median [1] following a diurnal pattern (i.e. the load reaches its peak
 535 during daytime hours), as shown in Figure 4.

536 We collected the VM resource demand at a five second sampling rate.
 537 Upon each VM placement, we determined the resource demand vector \overrightarrow{DV}
 538 by averaging the collected resource demand over the considered period using
 539 an exponential moving average, which makes the computation of the resource
 540 wastage vector \overrightarrow{WV} robust to workload demand oscillations.

541 The simulation aims to evaluate our dynamic VM placement algorithm
 542 using a large number of parameters and situations that are not easily repro-
 543 ducible in real life. Considering that the Google traces account for 29 days
 544 real execution, performing the same Pareto analysis using real experimenta-
 545 tion requires several years of execution. Apart from the workload injection,
 546 our algorithm uses precise resource information with no stochastic variables
 547 involved, indicating that the simulation matches the real execution.

548 7.2. Evaluation metrics

549 We use five metrics in our experimental evaluation:

- 550 • *Total energy consumption* accounts for the CPU power consumption P_p
 551 consumed by all PMs $p \in P_{used}$, considering CPU as the most energy
 552 consuming resource according to [20], proportional to its utilization [23]:

$$E = \sum_{p \in P_{used}} \int_0^{t_s} P_p(t) \cdot dt,$$

553 where: $P_p(t) = (P_p^{\max} - P_p^{\text{idle}}) + U_p(t) \cdot P_p^{\text{idle}}$, t_s is the simulation time, P_p^{\max}
 554 and P_p^{idle} are the power consumptions of the PM p at maximum and idle
 555 utilization levels (see Table 1), and $U_p(t)$ is p 's CPU utilization at instance
 556 t (i.e. complement of CPU component of wastage vector $\overrightarrow{WV}(p, t)$);

- 557 • *QoS violations* is the percentage of VMs that receive less resources than
558 their current demand relative to the entire simulation time;
- 559 • *Average number of active PMs* during the complete simulation;
- 560 • *Energy consumption of VM migration* is the energy consumed due to live
561 migrations (i.e. objective f_3 in Section 4.3). as a separate objective of our
562 study motivated in Section 1.2;
- 563 • *Average overcommitment ratio* is the average amount of resources allocated
564 in excess to the overall PM capacities (i.e. objective f_2 in Section 4.3).

565 7.3. Dynamic VM placement

566 We theoretically evaluated the adaptation of the dynamic VM placement
567 method by considering a decision making procedure triggered at the second,
568 ninth, and fourteenth hour of simulation, labeled as *Choice I*, *II*, and *III*.
569 Fig. 6 displays the Pareto frontiers obtained before and after each choice
570 using a two-dimensional graphical representation explained in Section 3.3.

571 *Choice I* (Fig. 6b) taken after the first hour of simulation incurs a higher
572 cost of migration leading to a low resource wastage. This placement results
573 in a reduction of the power consumption by up to 80% by turning 92 PMs to
574 a low power state (Fig. 7a). The consolidation of the VMs on the remaining
575 32 active PMs brings a 9% increase in QoS violations (Fig. 7c), which may
576 result in a high penalty for the Cloud provider under strict QoS requirements
577 As a consequence, the decision maker has the option to select a more energy
578 costly placement offering a better QoS.

579 *Choice II* (Fig. 6c) taken after the fourth hour of simulation incurs a
580 higher resources wastage and a lower overcommitment than the previous

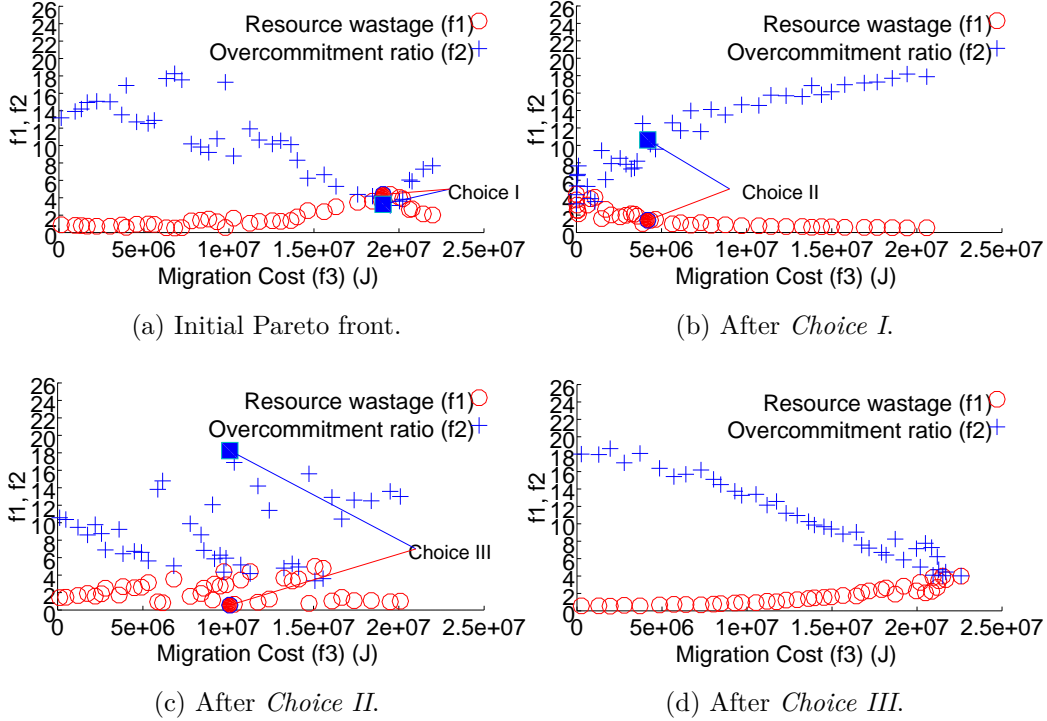
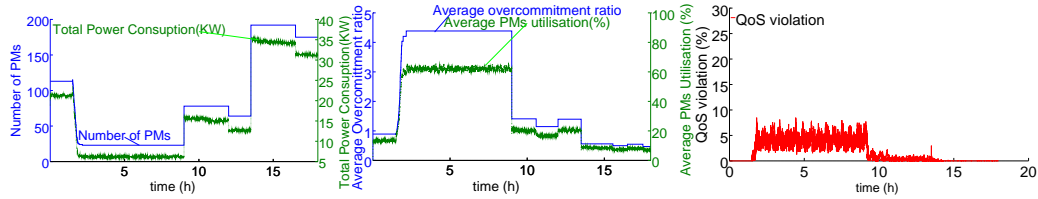


Figure 6: Pareto frontier generated by different VM tradeoff placements.

581 placement. Fig. 7c shows that the lower overcommitment ratio reduces the
 582 QoS violations to 1.2%, however, the utilization drops to 20% due to fewer
 583 consolidated VMs onto the same PM (Fig. 7b).

584 *Choice III* (Fig. 6d) taken after the ninth hour of simulation further
 585 increases the resources wastage. All 200 PMs present in the data center
 586 become active (Fig. 7a) and the power consumption increases by 130%. Fig.
 587 7c shows the benefit on QoS of this rather expensive choice.

588 Following our experiments, we observe that for an overall resource load
 589 below 80%, at most 10% of maximum number of VMs are migrated, with
 590 peaks of 40% when system is fully loaded, as typical in other setups which



(a) Power consumption versus active PMs. (b) Overcommitment ratio versus resource wastage. (c) QoS violations.

Figure 7: VM provisioning metrics after each tradeoff placement from Fig. 6.

591 exhibit similar load patterns [21]. In most cases, however, number of VM
 592 migrations is between 3 – 10% of the maximum number of VMs, which has
 593 a limited impact on performance (i.e. QoS violations).

594 7.4. Island NSGA-II

595 We compare in this section the Island NSGA-II algorithm against two
 596 state-of-the-art VM placement algorithms presented in Section 2.1:

- 597 • FFD as a baseline comparison method used by nearly all related works in
 598 evaluating their VM consolidation algorithms. We employ FFD by placing
 599 VMs according to their resource demand rather than request.
- 600 • MM_MBFD as one of the most cited and most recent dynamic placement
 601 algorithms in the literature that considers a trade-off between QoS and
 602 energy consumption metrics, similar to us;
- 603 • MM_MBDF_2 as our own extension to MM_MBFD that includes memory
 604 utilization for a fair comparison, not considered in the original version [7].
 605 We experimented with different MM_MBDF and MM_MBDF_2 upper and
 606 lower thresholds with a 30% difference.

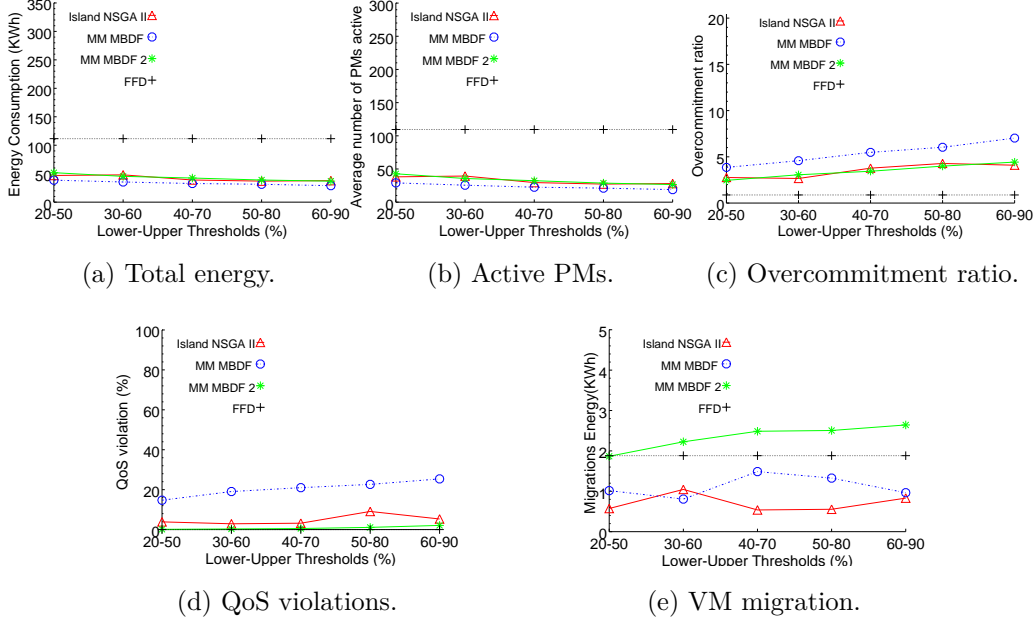


Figure 8: Simulation results for homogeneous data center.

607 As these algorithms generate a single placement instead of a Pareto frontier,
 608 tier, we cannot consider multi-objective metrics such as the hypervolume [4]
 609 in their comparison. For a fair comparison of a single tradeoff placement,
 610 we select the solution on the Pareto frontier closest to MM_MBDF_2 that,
 611 similar to us, considers both memory and CPU utilization in its optimization.

612 Among the most recent related works (see Section 2), we do not consider
 613 the ACO-based approach in [14] because it focuses only on reducing power
 614 consumption, rather than on finding trade-off solutions. Similarly, we do not
 615 compare our method with [30], as it optimizes the offline VM placement.

616 *7.4.1. Homogeneous data center (200 PMs of type M2)*

617 MM_MBDF reduced the total energy consumption by 21% in average
618 compared to Island NSGA-II (see Fig. 8a) by exclusively placing VMs accord-
619 ing to their CPU demand and overcommitting the memory, which lowering the
620 number of active PMs by 30% (see Fig. 8b). Fig. 8c shows that MM_MBDF
621 achieved an overcommitment ratio 48% higher than MM_MBDF_2 in aver-
622 age, and 45% higher than Island NSGA-II. The side effect is an increase
623 in QoS violations, as displayed in Fig. 8d. MM_MBDF_2 reduced the QoS
624 violations by 20% in average compared to MM_MBDF by jointly consider-
625 ing both CPU and memory demands. Island NSGA-II performed close to
626 MM_MBDF_2 with respect energy consumption (see Fig. 8a), average active
627 PMs (see Fig. 8b), and overcommitment ratio (see Fig. 8c). With respect to
628 QoS, Fig. 8d shows that Island NSGA-II exhibited the same level of violations
629 as MM_MBDF_2 in low-consolidated scenarios, and deviated by no more than
630 6% in high-consolidated ones. In addition, it reduced the migration cost by
631 70% compared to MM_MBDF_2, by 40.6% compared to MM_MBDF, and
632 by 64% compared to FFD (see Fig. 8e). Finally, FFD produced energy-
633 inefficient placements consuming 110 kWh regardless of the lower and upper
634 thresholds, since it allocated VMs according to their static resource requests
635 that suffer from overprovisioning.

636 We conclude that MM_MBDF reduces the energy consumption while in-
637 curring higher QoS violations than its memory-aware version. On the other
638 hand, Island NSGA-II computes VM placements close in performance to
639 MM_MBDF_2, while decreasing the migration energy by up to 70%.

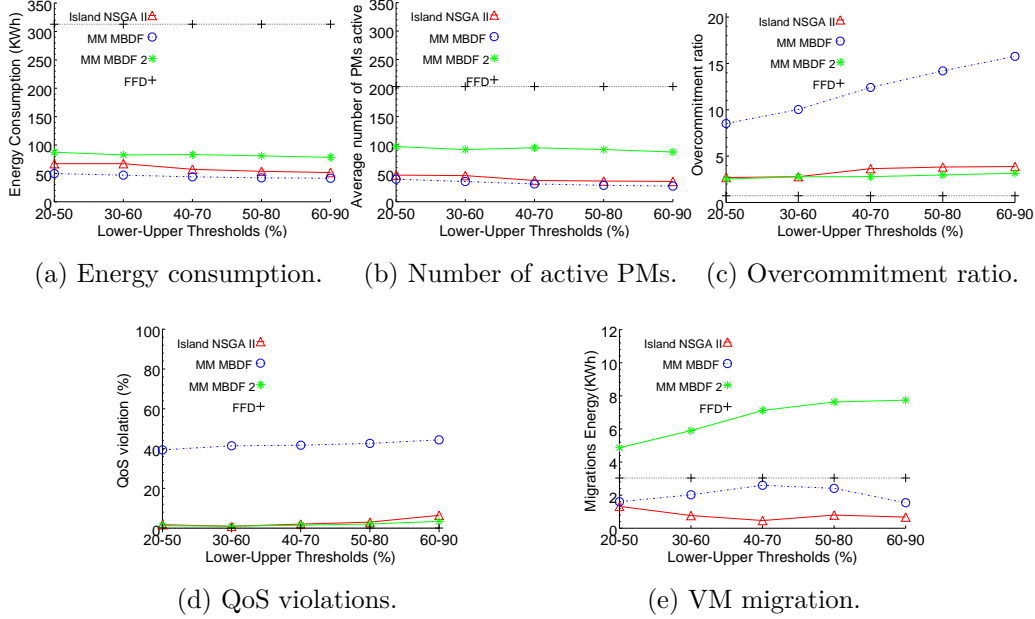


Figure 9: Simulation results for heterogeneous data center.

640 7.4.2. Heterogeneous data center (50 PMs of each type $M1 - M4$)

641 In the heterogeneous data center Island NSGA-II decreased the energy
642 consumption by 41% compared to MM_MBDF_2 and by 63% compared to
643 FFD (see Fig. 9a) by reducing the number of active PMs (see Fig. 9b), while
644 keeping the QoS violations below 6% (see Fig. 9d). Fig. 9b shows that Island
645 NSGA-II was able to use up to 50% less PMs than MM_MBDF_2, and up
646 to 75% less than FFD (Fig. 9b). Interestingly, Island NSGA-II achieved
647 an energy consumption close to MM_MBDF by overcommitting 71% less
648 resources in average (see Fig. 9c) and bringing 40% less QoS violations (see
649 Fig. 9d). Finally, Island NSGA-II significantly reduced the migration energy
650 by 76% compared to MM_MBDF_2, by 38% compared to MM_MBDF, and
651 by 62% compared to FFD, similar to the homogeneous experiment.

652 8. Conclusions and Future Work

653 The effective tradeoff between resource wastage and overcommitment is
654 a challenging task, and essential for reducing the energy cost of operating a
655 data center while guaranteeing the QoS. A Cloud data center approaches this
656 challenge by placing VMs to the available PMs. This paper addresses this
657 complex research problem by bringing the following scientific contributions:
658 1) a multi-objective formulation of the dynamic VM placement problem that
659 uses resource wastage, overcommitment ratio, and migration cost to represent
660 the energy and QoS tradeoffs; 2) an island-based evolutionary meta-heuristic
661 to approximate the set of Pareto tradeoff VM placements; 3) a dynamic VM
662 placement algorithm which supports decision making operators in optimizing
663 VM placements according to energy and QoS constraints.

664 We demonstrated using real traces from a Google data center cluster that
665 single solution VM placement approaches, although very appealing to formu-
666 late, understand and apply, are not effective compared to our multi-objective
667 approach that approximates the Pareto optimal set that reveals uncovered
668 regions of resource wastage, overcomittment, and live migration tradeoffs.
669 Our algorithm is linear in complexity with the number of VMs and PMs
670 and does not necessarily require human intervention for selecting preferred
671 VM; placement tradeoffs from the Pareto frontier. A basic decision making
672 with constant complexity can simply consider “energy budgets” or QoS con-
673 straints projected onto the Pareto optimal set of tradeoff placements. More-
674 over, multi-objective optimization literature showed that approximating the
675 complete set of tradeoff solutions is in many cases cheaper than computing
676 a single solution due to different navigaton of the search space. The Island

677 NSGA-II heuristic demonstrates performance close to other approaches and
678 exhibits less than 6% more QoS violations, while significantly reducing the
679 migration energy consumption by 55% in a homogeneous data center, and
680 by 57% in a heterogeneous data center.

681 In future work, we intend to extend the dimensions of our problem by
682 taking into account network and disk resources. We also plan to research au-
683 tomated decision making strategies to automate the selection of the “best”
684 Pareto solution during the dynamic VM placement process. Another interest-
685 ing work is to understand the interplay between the placement optimization
686 interval and the data center overall dynamics, such as migration time and
687 PM transition latency to a different (i.e. normal, low) power state.

688 **Acknowledgements**

689 This work received funding from:

- 690 • European Union’s Horizon 2020 research and innovation programme,
691 grant agreement 825134, “Smart Social Media Ecosyststem in a Blockchain
692 Federated Environment (ARTICONF)”;
- 693 • Austrian Science Fund (FWF), grant agreement Y 904 START-Programm
694 2015, “Runtime Control in Multi Clouds (RUCON)”;
- 695 • Austrian Agency for International Cooperation in Education and Re-
696 search (OeAD-GmbH) and Indian Department of Science and Tech-
697 nology (DST), project number, IN 20/2018, “Energy Aware Workflow
698 Compiler for Future Heterogeneous Systems”.

699 **References**

- 700 [1] D. Aikema, C. Kiddle, and R. Simmonds. Energy-cost-aware scheduling
701 of HPC workloads. In *2011 IEEE International Symposium on a World
702 of Wireless, Mobile and Multimedia Networks*, pages 1–7. IEEE, 2011.
- 703 [2] S. Akiyama, T. Hirofuchi, and S. Honiden. Evaluating impact of live mi-
704 gration on data center energy saving. In *6th International Conference on
705 Cloud Computing Technology and Science*, pages 759–762. IEEE, 2014.
- 706 [3] S. Akoush, R. Sohan, A. Rice, A. W. Moore, and A. Hopper. Predicting
707 the performance of virtual machine migration. In *2010 IEEE Interna-
708 tional Symposium on Modeling, Analysis and Simulation of Computer
709 and Telecommunication Systems*, pages 37–46, 2010.
- 710 [4] C. L. Bajaj, V. Pascucci, G. Rabbio, and D. R. Schikore. Hypervolume
711 visualization: a challenge in simplicity. In *IEEE Symposium on Volume
712 Visualization*, pages 95–102. IEEE, 1998.
- 713 [5] P. Barham, B. Dragovic, K. Fraser, S. Hand, T. Harris, A. Ho, R. Neuge-
714 bauer, I. Pratt, and A. Warfield. Xen and the art of virtualization. *ACM
715 SIGOPS Operating Systems Review*, 37(5e):164–177, 2003.
- 716 [6] S. A. Baset, L. Wang, and C. Tang. Towards an understanding of over-
717 subscription in cloud. In *2nd USENIX Workshop on Hot Topics in
718 Management of Internet, Cloud, and Enterprise Networks and Services*,
719 page 7. USENIX Association, 2012.

- 720 [7] A. Beloglazov, J. Abawajy, and R. Buyya. Energy-aware resource al-
721 location heuristics for efficient management of data centers for cloud
722 computing. *Future Generation Computer Systems*, 28(5):755–768, 2012.
- 723 [8] N. M. Calcavecchia, O. Biran, E. Hadad, and Y. Moatti. VM placement
724 strategies for cloud scenarios. In *IEEE 5th International Conference on*
725 *Cloud Computing*, pages 852–859. IEEE, 2012.
- 726 [9] R. N. Calheiros, R. Ranjan, and R. Buyya. Virtual machine provisioning
727 based on analytical performance and QoS in cloud computing environ-
728 ments. In *2011 International Conference on Parallel Processing*, pages
729 295–304. IEEE, 2011.
- 730 [10] M. Dabbagh, B. Hamdaoui, M. Guizani, and A. Rayes. Toward energy-
731 efficient cloud computing: Prediction, consolidation, and overcommit-
732 ment. *Network, IEEE*, 29(2):56–61, 2015.
- 733 [11] K. Deb, A. Pratap, S. Agarwal, and T. Meyarivan. A fast and eli-
734 tist multiobjective genetic algorithm: NSGA-II. *IEEE Transactions on*
735 *Evolutionary Computation*, 6(2):182–197, 2002.
- 736 [12] J. J. Durillo, A. J. Nebro, C. A. C. Coello, F. Luna, and E. Alba. A com-
737 parative study of the effect of parameter scalability in multi-objective
738 metaheuristics. pages 1893–1900, April 2008.
- 739 [13] T. Fahringer, R. Prodan, R. Duan, J. Hofer, F. Nadeem, F. Nerieri,
740 S. Podlipnig, J. Qin, M. Siddiqui, H.-L. Truong, A. Villazón, and
741 M. Wicczorek. ASKALON: A development and grid computing envi-
742 ronment for scientific workflows. In I. J. Taylor, E. Deelman, D. B.

- 743 Gannon, and M. Shields, editors, *Workflows for e-Science*, pages 450–
744 471. Springer, 2007.
- 745 [14] M. H. Ferdous, M. Murshed, R. N. Calheiros, and R. Buyya. Virtual
746 machine consolidation in cloud data centers using aco metaheuristic. In
747 *Euro-Par 2014 Parallel Processing*, pages 306–317. Springer, 2014.
- 748 [15] D. S. Johnson. *Encyclopedia of Algorithms*, chapter Vector Bin Packing,
749 pages 1–6. Springer, 2008.
- 750 [16] P. Lama and X. Zhou. aMoss: Automated multi-objective server provi-
751 sioning with stress-strain curving. In *2011 International Conference on*
752 *Parallel Processing*, pages 345–354. IEEE, 2011.
- 753 [17] J. Z. Li, M. Woodside, J. Chinneck, and M. Litoiu. CloudOpt: multi-
754 goal optimization of application deployments across a cloud. In *7th*
755 *International Conference on Network and Services Management*, pages
756 162–170. IFIP, 2011.
- 757 [18] H. Liu, H. Jin, C.-Z. Xu, and X. Liao. Performance and energy modeling
758 for live migration of virtual machines. *Cluster Computing*, 16(2):249–
759 264, 2013.
- 760 [19] V. D. Maio, G. Kecskemeti, and R. Prodan. A workload-aware energy
761 model for virtual machine migration. In *IEEE International Conference*
762 *on Cluster Computing*, pages 274–283. IEEE, 2015.
- 763 [20] K. T. Malladi, F. A. Nothaft, K. Periyathambi, B. C. Lee, C. Kozyrakis,
764 and M. Horowitz. Towards energy-proportional datacenter memory with

- 765 mobile dram. In *2012 39th Annual International Symposium on Com-*
766 *puter Architecture*, pages 37–48. IEEE, 2012.
- 767 [21] C. Mastroianni, M. Meo, and G. Papuzzo. Self-economy in cloud
768 data centers: Statistical assignment and migration of virtual machines.
769 In *Euro-Par 2011 Parallel Processing*, volume 6852, pages 407–418.
770 Springer, 2011.
- 771 [22] H. Mi, H. Wang, G. Yin, Y. Zhou, D. Shi, and L. Yuan. Online self-
772 reconfiguration with performance guarantee for energy-efficient large-
773 scale cloud computing data centers. In *2010 IEEE International Con-*
774 *ference on Services Computing*, pages 514–521. IEEE, 2010.
- 775 [23] L. Minas and B. Ellison. *Energy efficiency for information technology:*
776 *How to reduce power consumption in servers and data centers*, volume
777 pre. Intel Press, 2009.
- 778 [24] M. Mishra and A. Sahoo. On theory of VM placement: Anomalies in
779 existing methodologies and their mitigation using a novel vector based
780 approach. In *2011 IEEE International Conference on Cloud Computing*,
781 pages 275–282. IEEE, IEEE Computer Society, 2011.
- 782 [25] A. Murtazaev and S. Oh. Sercon: Server consolidation algorithm using
783 live migration of virtual machines for green computing. *IETE Technical*
784 *Review*, 28(3):212–231, 2011.
- 785 [26] V. Nae, A. Iosup, and R. Prodan. Dynamic resource provisioning in
786 massively multiplayer online games. *IEEE Transactions on Parallel and*
787 *Distributed Systems*, 22(3):380–395, 2011.

- 788 [27] J. Nieh, C. Vaill, and H. Zhong. Virtual-time round-robin: An $O(1)$
789 proportional share scheduler. In *USENIX Annual Technical Conference*,
790 pages 245–259. USENIX Association, 2001.
- 791 [28] S. Ostermann, K. Plankensteiner, and R. Prodan. Using a new event-
792 based simulation framework for investigating resource provisioning in
793 clouds. *Scientific Programming*, 19(2-3):161–178, 2011.
- 794 [29] C. Reiss, A. Tumanov, G. R. Ganger, R. H. Katz, and M. A. Kozuch.
795 Heterogeneity and dynamicity of clouds at scale: Google trace analysis.
796 In *Third ACM Symposium on Cloud Computing*, page 7. ACM, 2012.
- 797 [30] A. Sallam and K. Li. A multi-objective virtual machine migration policy
798 in cloud systems. *The Computer Journal*, 57(2):195–204, 2014.
- 799 [31] A. Strunk and W. Dargie. Does live migration of virtual machines cost
800 energy? In *27th International Conference on Advanced Information*
801 *Networking and Applications*, pages 514–521. IEEE, March 2013.
- 802 [32] S. Takahashi, A. Takefusa, M. Shigeno, H. Nakada, T. Kudoh, and
803 A. Yoshise. Virtual machine packing algorithms for lower power con-
804 sumption. In *4th International Conference on Cloud Computing Tech-*
805 *nology and Science*, pages 161–168. IEEE Computer Society, 2012.
- 806 [33] H. N. Van, F. D. Tran, and J.-M. Menaud. Performance and power
807 management for cloud infrastructures. In *3rd International Conference*
808 *on Cloud Computing*, pages 329–336. IEEE, 2010.
- 809 [34] A. Verma, P. Ahuja, and A. Neogi. pMapper: power and migration

- 810 cost aware application placement in virtualized systems. In *Middleware*
811 *2008*, pages 243–264. Springer, 2008.
- 812 [35] J. Wilkes and C. Reiss. ClusterData2011. [https://github.com/
813 google/cluster-data/blob/master/ClusterData2011_2.md](https://github.com/google/cluster-data/blob/master/ClusterData2011_2.md).
- 814 [36] M. Xu, L. Cui, H. Wang, and Y. Bi. A multiple QoS constrained schedul-
815 ing strategy of multiple workflows for cloud computing. In *Parallel and
816 Distributed Processing with Applications, 2009 IEEE International Sym-
817 posium on*, pages 629–634. IEEE, 2009.